



2016-11-30

# Determining the Index of Refraction of Aluminum Fluoride in the Ultra Violet Spectrum

Zoe Hughes  
zhughes@drew.edu

Follow this and additional works at: <https://scholarsarchive.byu.edu/studentpub>

 Part of the [Astrophysics and Astronomy Commons](#)

---

## BYU ScholarsArchive Citation

Hughes, Zoe, "Determining the Index of Refraction of Aluminum Fluoride in the Ultra Violet Spectrum" (2016). *All Student Publications*. 187.

<https://scholarsarchive.byu.edu/studentpub/187>

This Report is brought to you for free and open access by BYU ScholarsArchive. It has been accepted for inclusion in All Student Publications by an authorized administrator of BYU ScholarsArchive. For more information, please contact [scholarsarchive@byu.edu](mailto:scholarsarchive@byu.edu), [ellen\\_amatangelo@byu.edu](mailto:ellen_amatangelo@byu.edu).

# Determining the Refractive Index of Aluminum Fluoride (AlF<sub>3</sub>)

Research Experience for Undergraduates (REU Program)  
Brigham Young University  
Physics and Astronomy Department  
Provo, Utah

Zoe Hughes  
Mentor: Dr. R. Steven Turley  
Project Funded by: NSF-1461219  
August 12, 2016

**Abstract:** A NASA project called Large UV/Optical/Infrared Surveyor (LUVOIR) is looking into ways to coat a mirror for a new space telescope. We contributed to this project by investigating aluminum fluoride (AlF<sub>3</sub>) as a possible coating for the mirror. We measured the index of refraction of AlF<sub>3</sub> in the wavelength range 6 – 49.5 nm by testing three sample mirrors, each made up of a silicon wafer with a coating of AlF<sub>3</sub>. We took data at the Advanced Light Source (ALS) in Berkeley, California and in the laboratory at Brigham Young University (BYU). There are discrepancies between the measurements from ALS and BYU. The cause of these differences is still unknown, but we have concluded the ALS measurements are more reliable. The optical constants found at the ALS agree with index of refraction data taken from The Center for X-Ray Optics (CXRO) for AlF<sub>3</sub>.

## Acknowledgements

I would like to thank Dr. Turley for mentoring me this summer and giving me an unforgettable experience. His welcoming attitude and patient teaching are skills not to be taken for granted.

Also, I appreciate Dr. Allred for allowing me some of his time and helping me through the analysis. A special thanks to Margaret Miles who helped me immensely throughout the summer and was one of the reasons I enjoyed this research so much. I would also like to acknowledge the

Brigham Young University Physics REU program and National Science Foundation- Grant

1461219 for funding my project.

# Table of Contents

<b>1. Introduction</b>	<b>1</b>
<b>1.1 Motivation</b>	<b>1</b>
<b>1.2 Background</b>	<b>2</b>
<b>1.3 Theory</b>	<b>3</b>
<b>2. Methods</b>	<b>5</b>
<b>2.1 Setup</b>	<b>6</b>
<b>2.2 ALS</b>	<b>7</b>
2.2.1 Collecting Data	7
<b>2.3 BYU</b>	<b>12</b>
2.3.1 Alignment	12
2.3.2 Collecting Data	12
<b>3. Results</b>	<b>13</b>
<b>3.1 ALS Data Analysis</b>	<b>13</b>
3.1.1 Comparison with CXRO Data	14
3.1.2 Modify Model: Thickness	16
3.1.3 Modify Model: Add a Layer	18
<b>3.2 ALS and BYU Data Comparison</b>	<b>20</b>
<b>3.3 Conclusion and Future Work</b>	<b>23</b>
<b>References</b>	<b>25</b>
<b>List of Figures</b>	<b>25</b>

# 1. Introduction

In the field of Extreme Ultraviolet Optics, scientists work with light of extremely short wavelengths, approximately 10 nm to 124 nm. They are interested in how extreme ultraviolet (EUV) light interacts with different materials. EUV light is invisible to the human eye. On earth, some sources of this light can be accelerated electrons or plasma. In space, the Sun emits light from a wide range of wavelengths, including EUV. The interaction between EUV light and space telescopes have led to the capture of magnificent images, like the ones taken by the Hubble telescope. Space telescopes require mirrors that are durable under the harsh conditions of space and are able to work with a range of different wavelengths. Depending on the objectives of the space mission, scientists may want a mirror that maximizes or minimizes the reflectance of various wavelengths. Therefore, the mirror must be designed to have specific optical properties for extreme ultraviolet light.

## 1.1 Motivation

The motivation for this project first begins with NASA's Large UV/Optical/Infrared Surveyor (LUVOIR) project. NASA's project aims to send a telescope into space to explore new stars and galaxies, which will further the study of astrophysics and exoplanets. The LUVOIR space telescope will have a mirror that will be approximately 16 meters in diameter and have optical properties for EUV light. Aluminum is commonly used for mirrors; however, when it is exposed to the atmosphere it oxidizes, which greatly reduces its ability to reflect EUV light. The research team at Brigham Young University (BYU) is one of many teams across the country investigating different ways to coat the mirror to protect the aluminum. The BYU team is made up of two groups: one group designs the mirror and the second group tests the mirror's optical

properties with EUV light. The project discussed in this paper involves the work of the second group. One coating we are looking into is aluminum fluoride ( $\text{AlF}_3$ ). One of the objectives of this project is to determine if  $\text{AlF}_3$  is the appropriate match for the LUVOIR telescope mirror.

The second objective for this project is to uncover new information about  $\text{AlF}_3$ . This compound has been used on other mirrors before and has proven to be an excellent coating to reflect short wavelengths (more information on the previous studies is discussed in section 1.2). In contrast to the previous studies, this project uses light of shorter wavelengths, from 6 nm to 49.5 nm. Optical properties in this wavelength range have never been found experimentally for  $\text{AlF}_3$ . Hence, another purpose for this project is to calculate the index of refraction of  $\text{AlF}_3$  in the EUV spectrum.

## 1.2 Background

Aluminum fluoride is selected as the coating for this project because it has shown promise in previous studies. For instance, at the University of Colorado, Boulder, scientists studied the optical properties of atomic layer deposited  $\text{AlF}_3$  films for wavelengths from 90 nm to 800 nm [1]. Similar to the way the samples at BYU were designed, the scientists added a layer of  $\text{AlF}_3$  to a silicon wafer. Silicon wafers are used because they serve as a smooth base layer and have a known structure. They measured the reflectance at two incident angles, 10 and 45 degrees, and concluded that their results roughly matched their predicted values and also findings of another study done in France [1].

This study was done at Charles Fabry Laboratory of the Optics Institute focused on finding the optical constants of  $\text{MgF}_2$  and  $\text{AlF}_3$  [2]. These scientists, F. Birdou et al, used light from 60 nm to 124 nm. They concluded that  $\text{AlF}_3$  is a unique compound for shorter wavelengths because its extinction coefficient is considerably lower than  $\text{MgF}_2$ . This means  $\text{AlF}_3$  does not

absorb light of shorter wavelengths as strongly as  $\text{MgF}_2$  [2]. This study is a good reference for our results as well. Furthermore, due to previous research, especially the two examples mentioned,  $\text{AlF}_3$  is chosen because there is evidence to indicate it can effectively reflect EUV light.

### 1.3 Theory

This project involves the interaction of light with thin films. Therefore, before an explanation can be given of how to determine the index of refraction, an understanding of what this optical constant is and how light behaves must be established. To begin, when light makes contact with a new material the speed of the waves changes. The index of refraction indicates how light will propagate through a given medium. This optical constant is complex:

$$N = n + ik \quad (1).$$

The real component,  $n$ , is inversely proportional to the phase velocity, or the velocity at which the crests of the waves propagate. The equation

$$n = \frac{c}{v} \quad (2),$$

illustrates this, where  $n$  is the real index of refraction,  $v$  is the speed of the wave, and  $c$  is the speed of light. The imaginary component,  $k$ , describes the loss of the light wave due to absorption. Another equation for the index of refraction is:

$$N = (1 - \delta) + i\beta \quad (3).$$

In this form, the imaginary component is referred to as  $\beta$ , and the real part,  $n$ , is written as  $(1 - \delta)$ . Also note that  $\delta = (1 - n)$ .

A material can speed up or slow down a wave. For instance, if the light wave travels from a lower index of refraction to a higher one, then the speed decreases. On the other hand, if the wave travels from a higher index of refraction to a lower one, then the speed increases, but of

course never past the speed of light [3]. Not only does the speed of the waves change when they enter a new medium, but they also refract. The refraction of light follows Snell's law that relates the angle of incident light and index of refraction of the first medium to the angle of refraction and the index of refraction of the second medium [3]:

$$n_1 \sin \theta_{incidence} = n_2 \sin \theta_{refraction} \quad (4).$$

Snell's law makes use of only the real part of the index of refraction. Figure 1 demonstrates the paths of refraction and reflection of light when incident on a new medium.

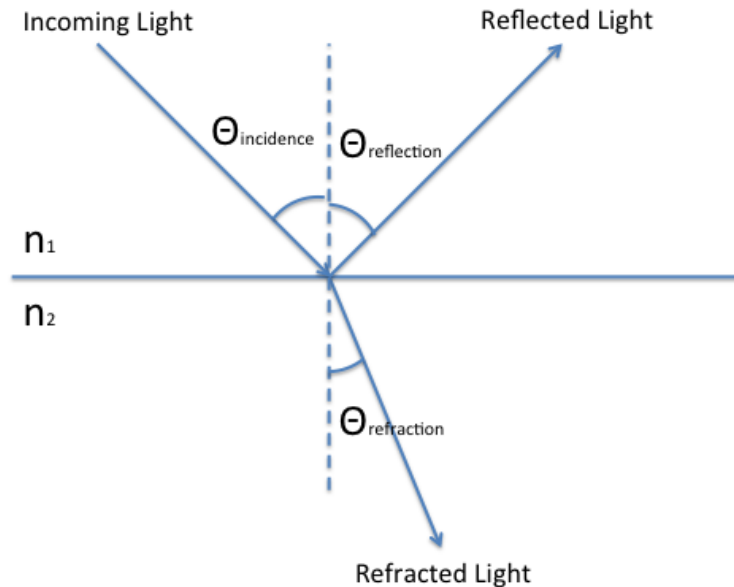


Figure 1: Snell's Law and the Law of Reflection. When light is incident on a new surface, it may refract and reflect. The refracted light obeys Snell's Law and the reflected light obeys the Law of Reflection that says the angle of incidence is equal to the angle of reflection.

Note that the light in this figure is traveling from a smaller to larger index of refraction because the refracted light bends toward the normal. If the light went from a larger to smaller index, then the light would bend away from the normal. Not all of the light refracts through the material. Some of the light does not enter the medium at all and instead reflects off of it.

The reflection of light follows the Law of Reflection:

$$\theta_{incidence} = \theta_{reflection} \quad (5).$$

As seen in Figure 1, the angle of incoming light measured relative to the normal is equal to the angle of the reflected light, also relative to the normal. The amount of light that is transmitted and reflected through a material is based on the Fresnel coefficients:

$$r_s = \frac{E_r(s)}{E_i(s)} = \frac{n_i \cos \theta_i - n_t \cos \theta_t}{n_i \cos \theta_i + n_t \cos \theta_t} \quad (6)$$

$$t_s = \frac{E_t(s)}{E_i(s)} = \frac{2n_i \cos \theta_i}{n_i \cos \theta_i + n_t \cos \theta_t} \quad (7)$$

$$r_p = \frac{E_r(p)}{E_i(p)} = \frac{n_i \cos \theta_i - n_t \cos \theta_t}{n_i \cos \theta_i + n_t \cos \theta_t} \quad (8)$$

$$t_p = \frac{E_t(p)}{E_i(p)} = \frac{2n_i \cos \theta_i}{n_i \cos \theta_i + n_t \cos \theta_t} \quad (9).$$

The Fresnel coefficients indicate how much of the incident light is transmitted or reflected. Reflectance is the ratio of the reflected amplitude of the electric field to the incident amplitude of the electric field. Transmittance is the ratio of the transmitted to the incident amplitude of the electric field. The reflection and transmission of light are dependent on the index of refraction and angle of incidence. The subscripts  $s$  and  $p$  denote the polarization:  $s$  represents the perpendicular polarization and the  $p$  represents the parallel polarization [3]. When measuring the index of refraction, it is essential to know how light reflects and refracts. Although we cannot see the EUV light's path, we know how it will interact with our sample.

## 2. Methods

We took measurements at the Advanced Light Source (ALS) at Lawrence Berkeley National Laboratory in California as well as in our own laboratory at Brigham Young University. We only had a limited time at the ALS, but fortunately we were able to retake data at BYU and compare it with our first set of measurements. Although the setups are alike, the experience of taking the data at each lab varied a bit because we started with the alignment of the entire system

at BYU. The process of collecting the data was a simple task compared to the challenging process of aligning and configuring the system. Therefore, because the alignment was a fundamental step, it is discussed in detail in this chapter in addition to the methods of data collection.

## 2.1 Setup

The process of measuring the optical properties of a thin film begins with an EUV light source. Figure 2 illustrates the setup we have at BYU.

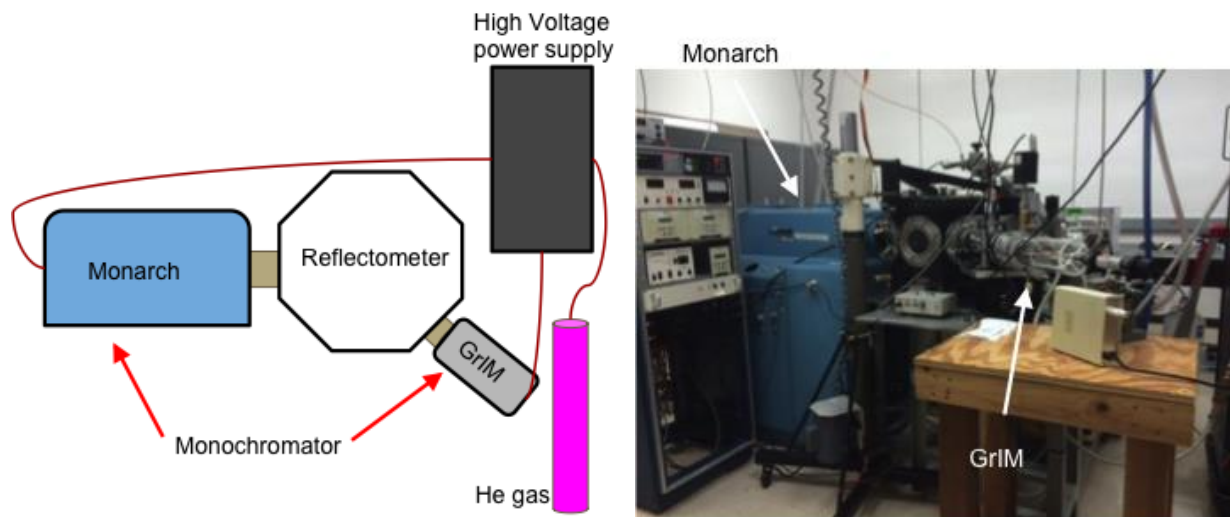


*Figure 2: BYU Setup.* There are two monochromators attached to the reflectometer. Monarch is used for longer EUV waves, while GrIM is used for shorter EUV waves. Each one is connected to a plasma source and works independently of the other.

To begin with, we ionize helium gas to make plasma. From the plasma source, the EUV light travels to the monochromator. We have two monochromators: Monarch and GrIM (Grazing Incidence Monochromator). A monochromator works by selecting one wavelength using a diffraction grating, which is typically made out of glass or metal. The diffraction grating has closely lined parallel grooves, and when set at different angles it separates the light and reflects only part of the spectrum. We typically use gratings with 300-600 lines/mm. From the

monochromator, the light then goes to the reflectometer, reflects off of the sample, and travels into the detector. We record the beam signal by measuring the current from the detector.

At the ALS, the setup also has a monochromator and a reflectometer; however, the EUV source is synchrotron radiation. The ALS accelerates electrons close to the speed of light and bends them into a circle with magnets. The photons emitted are used as the light source. This system is more powerful than the one at BYU because the incoming beam is more intense and is broadband, meaning it has a wider range of incident wavelengths to choose from.

## **2.2 ALS**

At the ALS, we tested three samples: A, C, and D. These three samples were recommended by the design group to be the most ideal to measure due to their smoothness. For each sample, we measured the index of refraction in three steps: 1) we used a range of wavelengths from 6 nm to 49.5 nm, and measured the reflectance vs. angle for each wavelength. The range of incident angles for the mirror was from 0 to 80 degrees. 2) We fitted the data to a model using Mathematica. For each sample, we ran the fit twice: the first to determine the thickness of the sample and the second to determine the index of refraction. 3) We graphed the index of refraction vs. wavelength for each sample.

### **2.2.1 Collecting Data**

To further explain the method of collecting data, the process for measuring sample A for one wavelength of 45 nm is clarified in detail. For the first step, in order to measure reflectance vs. incident angle, we measured three things: 1) the signal of the beam going straight to the detector without reflecting off of the mirror,  $I_0$ . 2) The signal of the beam during theta-2theta scans, which is when the mirror moves an angle theta and the detector must move exactly two times theta to collect as much light as possible. We moved the mirror from 0 to 80 degrees and

the detector from 0 to 160 degrees simultaneously, and recorded the signal from the detector called  $I_r$ . 3) Lastly, we measured the signal of the detector when no light is in the chamber. The detector still receives a low signal called dark current, DC. Dark current is the background noise from the amplifier and detector. We subtracted it from the reflected and incident radiation so it did not disrupt our measurements. Below is the equation for calculating reflectance:

$$R = \frac{\text{Reflected Radiation} - \text{Dark Current}}{\text{Incidence Radiation} - \text{Dark Current}} = \frac{I_r - DC}{I_o - DC} \quad (9)$$

The reflectance is a ratio of reflected radiation over the incident radiation. Figure 3 shows the result of these measurements through a reflectance vs. incident angle graph.

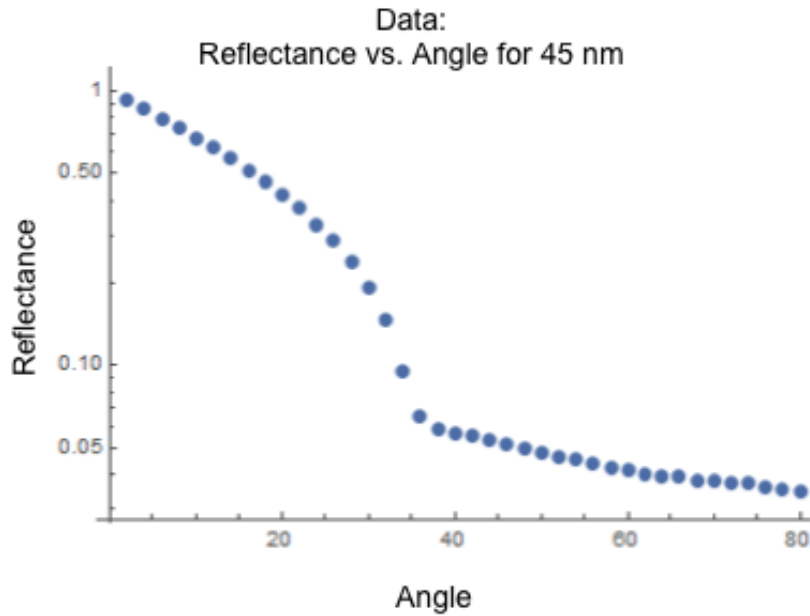
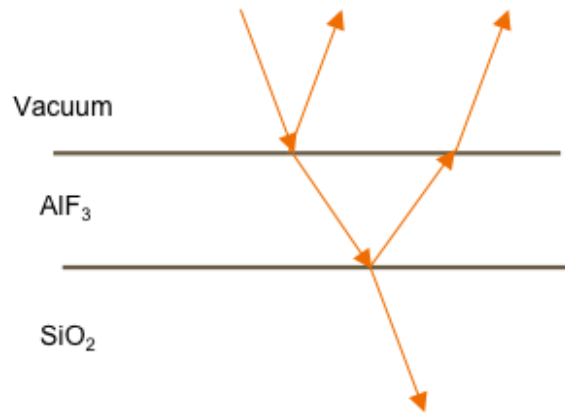


Figure 3: Reflectance vs. Incident Angle (degrees) for Sample A for 45 nm. This is a log graph, which displays the relationship more clearly. A graph like this was produced for every wavelength used on each sample.

This graph was constructed using Mathematica. As the incident angle with respect to grazing increases, the reflectance decreases. This shape of the graph indicates how the mirror was designed and the thickness of the  $\text{AlF}_3$ . A graph like Figure 3 was constructed for all the different wavelengths, so each sample has around ten graphs. Figure 4 illustrates the layers of our

samples. The samples have a layer of aluminum fluoride and then an underlying layer of silicon dioxide. The dip in the graph is caused by the light that reflects off of the layer of  $\text{SiO}_2$ , which is 180 degrees out of phase with the light reflecting off of the layer of  $\text{AlF}_3$ . For reference in Figure 4, the two beams of light traveling away from the  $\text{AlF}_3$  layer are 180 degrees out of phase.



*Figure 4: Layers of the Sample Mirror.* The bottom layer of the mirror is silicon dioxide, and then the aluminum fluoride film is on top. The light travels from the vacuum and reflects and refracts through the other two layers.

The second step of calculating the index of refraction is fitting the data to the model in Mathematica. This model is based off of the Fresnel coefficients and boundary conditions for reflection and transmission, which dictate how much light reflects off of and transmits through the sample. The model returns reflectance when given specific wavelengths and incident angles. It predicts the thickness of the sample and both the real and imaginary components of the index of refraction. The model is first run to predict the thickness of the sample. For each wavelength, a predicted thickness is given. Figure 5 shows the thickness vs. wavelength for sample A.

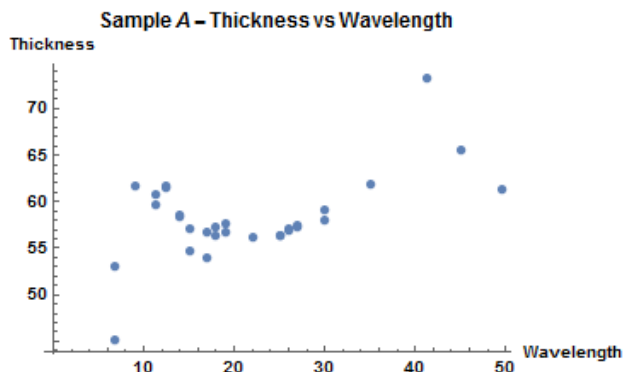


Figure 5: Thickness (Angstroms) vs. Wavelength (nm) for Sample A. The thickness values that clustered together from 12.5nm to 30nm were averaged. Graphs like Figure 5 were created for all of the samples to calculate the thickness.

An average of clustered values was taken to be the thickness for all of the wavelengths. For instance, for sample A we averaged thicknesses from 12.5 nm to 30 nm and calculated 57.42 Angstroms for the constant thickness for the whole sample.

Using the constant thickness from the first fit, the model is run a second time to predict the index of refraction. Figure 6 displays the graph comparison of the data and model for sample A at a wavelength of 45 nm.

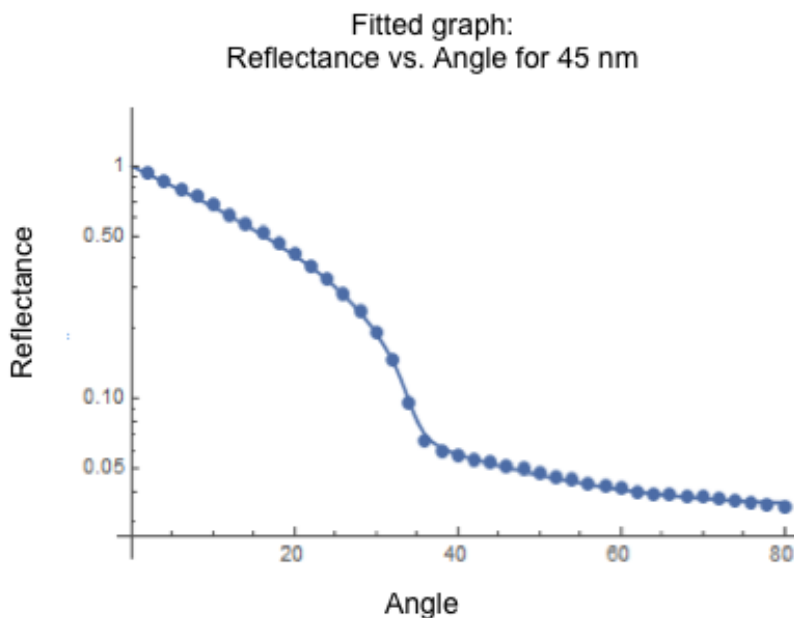


Figure 6: Fitted Graph for Sample A at 45 nm. The dots represent the data and the line represents the model fit.

The fit for this wavelength agrees with the data because the fit represented by the line connects all of the data points. Unfortunately, not all fits came out as nice. As we reached the shorter wavelengths, the model and data points did not match up. Figure 7 illustrates this.

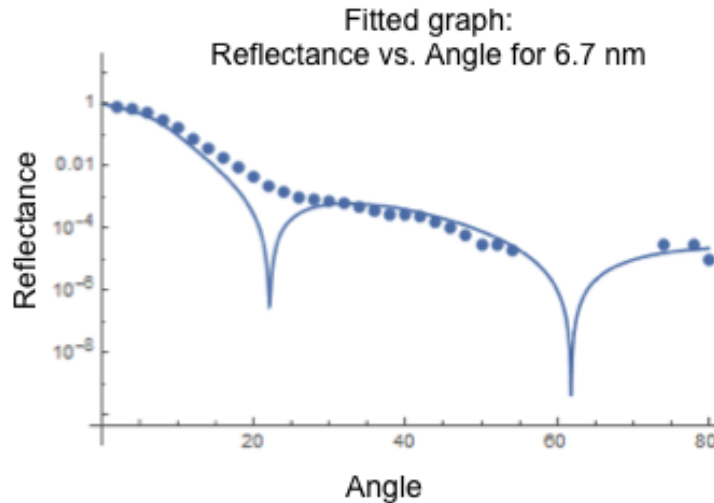


Figure 7: Fitted Graph for Sample A at 6.7 nm. This fit did not come out as well as the 45 nm. The data points are missing at some angles. The fit has two dips that are not present in the data.

When using shorter wavelengths, reasons for the poor fits are most likely the roughness of the sample and the dark current. Roughness can cause a problem because with shorter wavelengths a rough surface will matter more than if the wavelength is longer. The roughness will obstruct the light wave's path more and make it jiggle. Additionally, dark current might be an issue because when we take measurements for shorter wavelengths we increase the gain so we can see the signal better. However, when we increase the gain, we increase the dark current too, so it disrupts the measurements. Graphs like Figure 6 and 7 were done for every wavelength we used for each sample. Assembling all of these graphs, we can examine the relationship between the index of refraction and wavelength. These graphs will be discussed in the Results chapter in section 3.1.

## 2.3 BYU

### 2.3.1 Alignment

Before we were able to take data in the laboratory at BYU, we had to align the system. This process involved aligning the sample stage and the detector for the theta-2theta scans. Using an old sample mirror on the sample stage, we first did a rough alignment with a HeNe laser, and then a fine alignment with the plasma. Just like at the ALS, the theta-2theta scans are an essential part of measuring reflectance. When the mirror moves an angle theta, the detector must move twice the angle of theta to record accurate measurements. For each monochromator, we shined a laser down the path the plasma would take and adjusted the sample stage and the detector until they were aligned. Then we used the plasma as the light source. For the rough adjustment, we could see the laser and confirm alignment with our sight. However with the EUV light, we used the detector to indicate if the alignment was correct by reading the number of counts. In the reflectometer, there is a pinhole for the EUV light to direct the path to the detector. We aligned the pinhole and knew it was in the correct position by the highest count readings. After the system was correctly aligned, data collection could begin.

### 2.3.2 Collecting Data

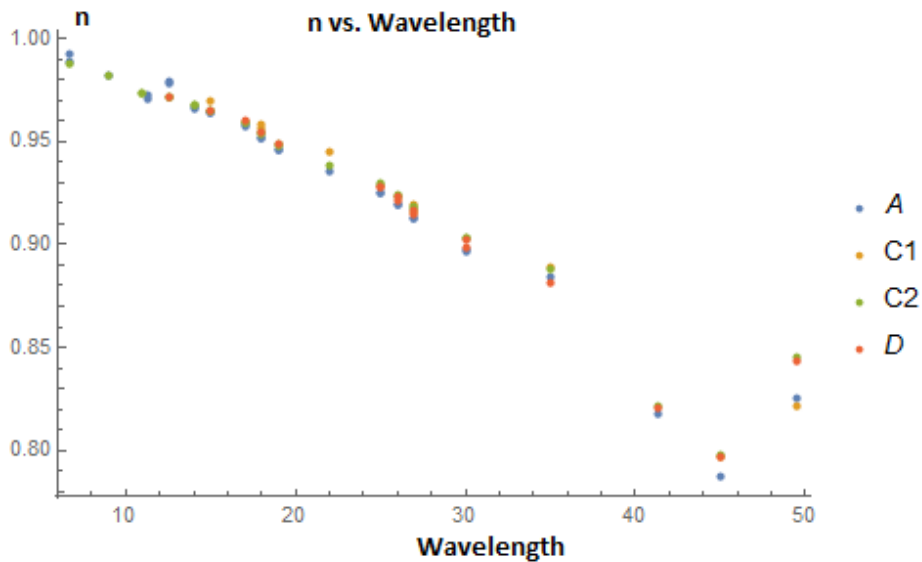
The procedure for taking measurements in the BYU lab is a bit more complex than the procedure at the ALS lab. Even though we do not have to worry about subtracting the dark current, we have to run multiple scans for one wavelength for every incident angle. At the ALS, we simply ran one scan for one wavelength that ranges through all incident angles 0 to 80 degrees. Also since the current of the plasma fluctuates,  $I_0$  scans (that measure the intensity of the incoming beam) must be taken every couple of runs. Because data collection is more time consuming, we only measured sample D at wavelengths 30.4nm and 25.6nm. Challenges

sometimes occurred with lighting the plasma. Additionally, the counts on the detector were not consistent. Some days we recorded better counts for the same wavelength than others. Due to low counts, we could only measure incident angles up to 40 degrees. At angles past 40 degrees, the counts were too low to record.

### 3. Results

#### 3.1 ALS Data Analysis

The relationship that we are ultimately interested in is the index of refraction versus the wavelength. From the reflectance measurements like Figures 6 and 7, we take the predicted real and imaginary index of refraction values from the model and graph both components vs. wavelength. We also want to know  $\delta$  vs. wavelength. Figure 8 illustrates these relationships.



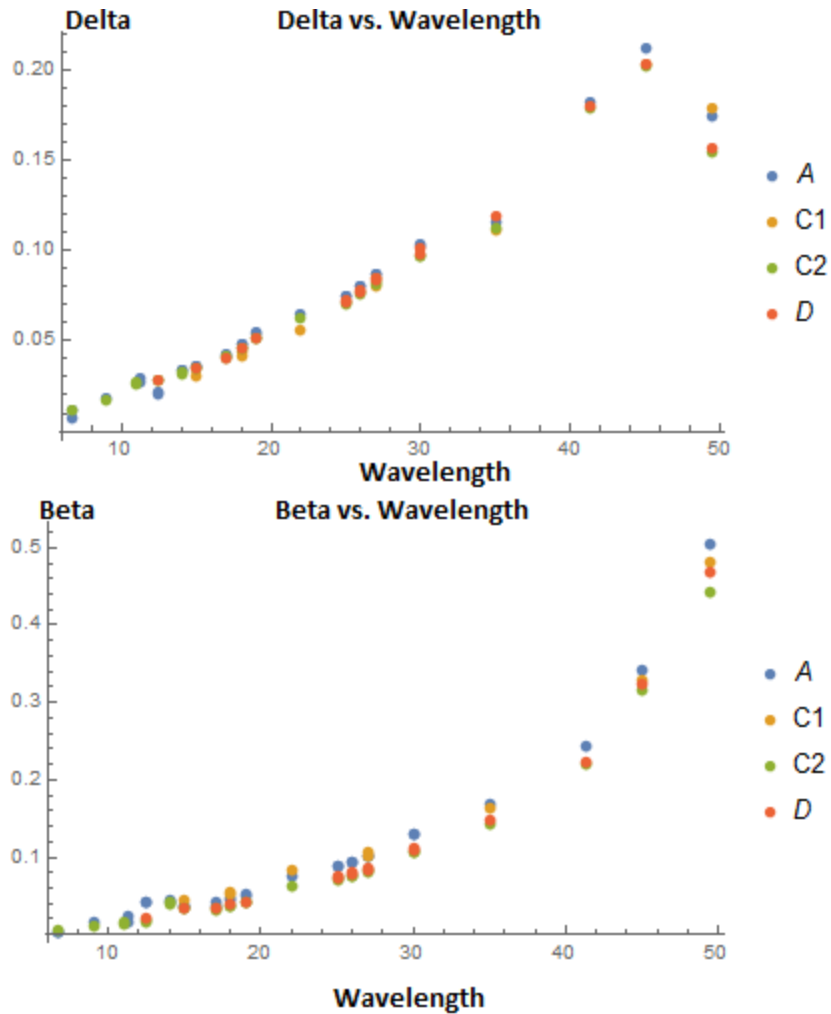


Figure 8: Graphs of  $n$ , Delta, and Beta vs. Wavelength (nm). These graphs compare the optical constants of the three samples A, C, and D. There is a C1 and C2 because sample C was measured on two separate days.

All three samples follow a similar trend in values for  $n$ ,  $\delta$  and  $\beta$ . Since these graphs are only the initial results, further analysis of the data needs to be done to test its accuracy. To accomplish this, we need to compare the data to known values of the index of refraction for  $\text{AlF}_3$  and then adjust the model to see if the fit can be improved.

### 3.1.1 Comparison with CXRO Data

A comparison of the ALS data with the known values of the index of refraction for  $\text{AlF}_3$  is shown in Figure 9.

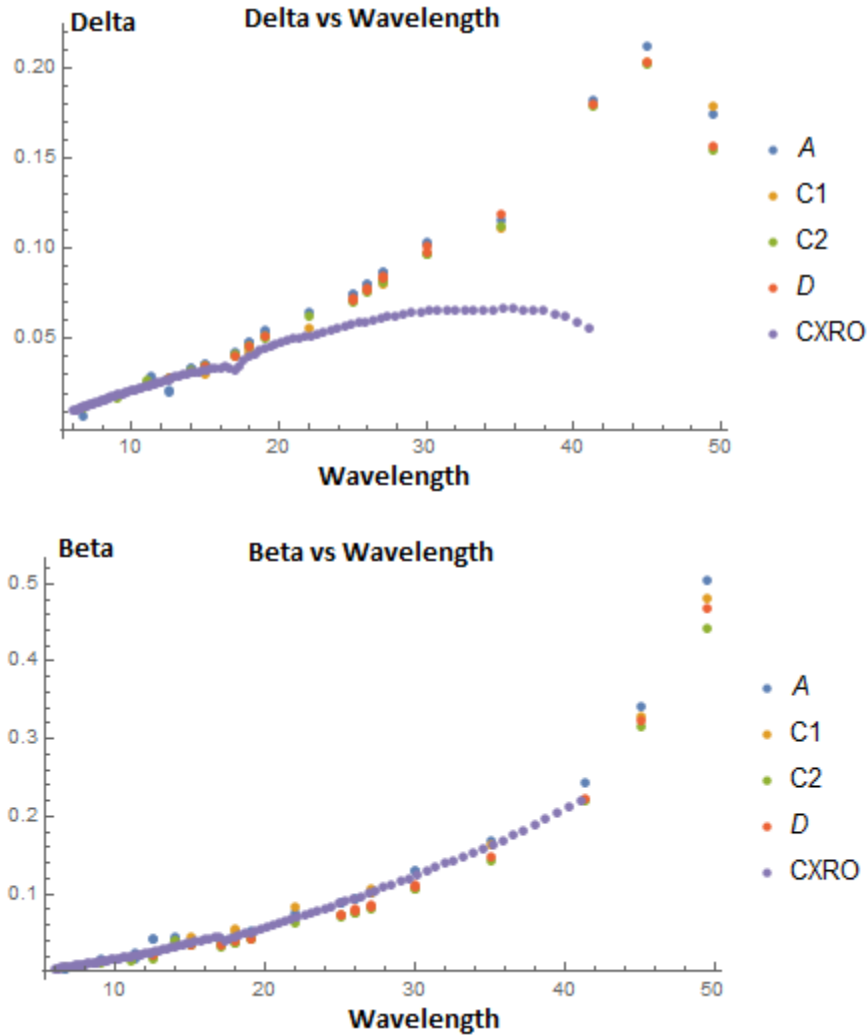


Figure 9: Comparison of Delta and Beta vs. Wavelength (nm) Graphs of ALS Data with CXRO Data.

The known values come from the CXRO (The Center for X-Ray Optics) website that provides the index of refraction for compounds from wavelengths 6 nm to 41.3 nm. The CXRO calculates the index of refraction by using the relationship that the index of refraction is proportional to density [4]. They use the properties of aluminum separately and then consider another known fluoride, for instance sodium fluoride. Utilizing the independent atom approximation, the index of refraction of aluminum fluoride can be determined from the fluoride and aluminum. (For more information on this process, see CXRO website reference [5].) Due to

this method of determining the refractive index, it is expected that our experimental values should closely agree with the values of the CXRO data for the shorter wavelengths. This is because the independent atom approximation for  $\text{AlF}_3$  is accurate for the inner electrons that are closely bound to the nucleus. However, this approximation is not correct for the outer electrons that are not tightly bound. This causes the CXRO data for the longer wavelengths to differ from experimental values. This prediction is confirmed in Figure 9. For the shorter wavelengths, values for  $\delta$  and  $\beta$  are close to the CXRO data, yet as seen in the  $\delta$  vs. wavelength graph, around 22 nm the data sets diverge. In the  $\beta$  vs. wavelength graph, the data sets are agreeable until the 41.3nm, which is as far as the CXRO data can go. This shows that our experimental data concurs with the CXRO data. The model fits well; however, the next step is to try to improve it through adjusting the model.

### 3.1.2 Modify Model: Thickness

The first adjustment we made is changing the thickness. Predictions of the sample thicknesses were made immediately after the creation of the samples. The following table in Figure 10 compares the thicknesses used in the first model (experimental thicknesses) and the predicted thicknesses. The predicted thicknesses were calculated through ellipsometry measurements.

Sample	Experimental Thicknesses (Angstroms)	1 <sup>st</sup> Predicted Thicknesses (Angstroms)	2 <sup>nd</sup> Predicted Thicknesses (Angstroms)
A	57.42	60.90	62.02
C	78.60 (Day 1)	88.90	93.54
	31.40 (Day 2)		
D	32.44	36.70	43.62

Figure 10: Table of the Thicknesses. The original model uses the experimental thicknesses and the modified model uses the first predicted thicknesses.

The experimental thicknesses are relatively close to the predicted thicknesses, except for sample C on day 2. We measured sample C on two separate days and calculated two completely different thicknesses. We concluded that this occurred because we chose an uneven spot on the mirror on the second day that did not have much aluminum fluoride. Figure 11 displays the graphs for this modified model using the first predicted thicknesses.

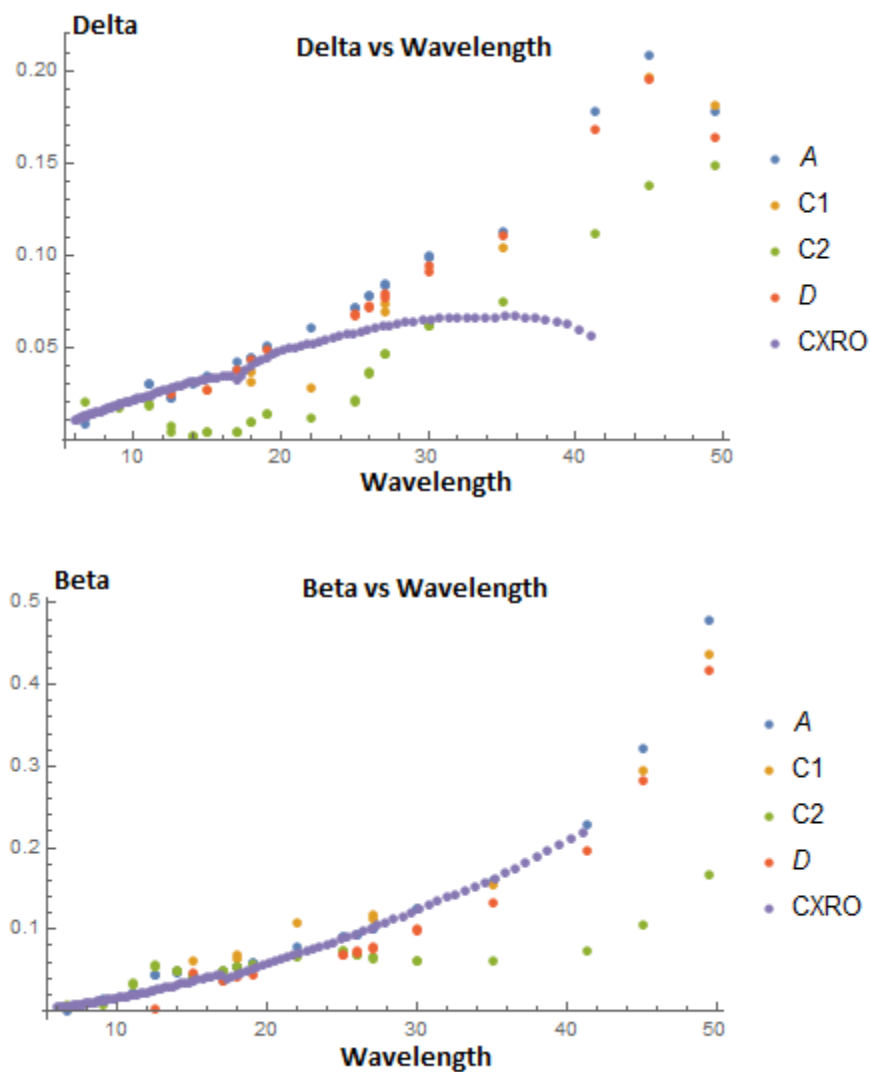


Figure 11: Graphs of Delta and Beta vs. Wavelength (nm) of the Data Modeled with the Predicted Thicknesses Compared to the CXRO Data.

Compared to the original fit, this modified fit spreads out the values for  $\delta$  and  $\beta$  more. Sample C2 does not match the CXRO data or the other samples, but this is expected because the experimental thickness is significantly off of the predicted value. There is a trend that sample A has the higher values for the longer wavelengths compared to the other samples. The data sets still diverge for  $\delta$  around 22 nm, like in the original model. Overall, the experimental data does not fit as well with the CXRO after this modification. We concluded that the experimental averages are more accurate than the predictions. The ellipsometry overestimated the thicknesses of the samples. Hence, changing the thickness did not improve the model.

### 3.1.3 Modify Model: Add a Layer

The second adjustment is adding another layer. During the construction of the sample, there was a concern of a leak that exposed the sample to more oxygen. This might have caused a layer of aluminum oxyfluoride to form under the aluminum fluoride. This means that the layer that was at first assumed to be pure  $\text{AlF}_3$  might actually be split into two layers  $\text{AlF}_2\text{O}$  and  $\text{AlF}_3$ . Figure 12 shows the new possible structure of the samples.

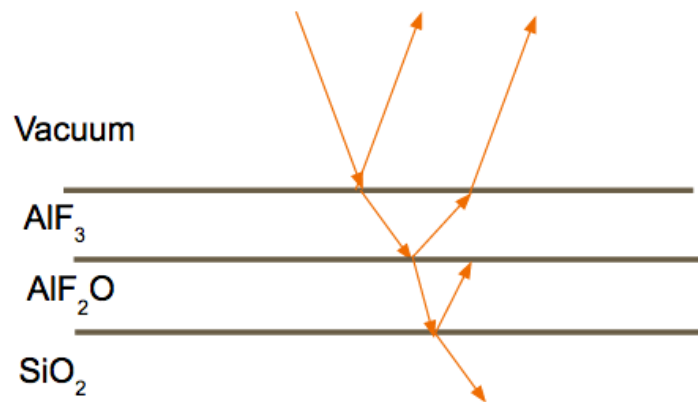
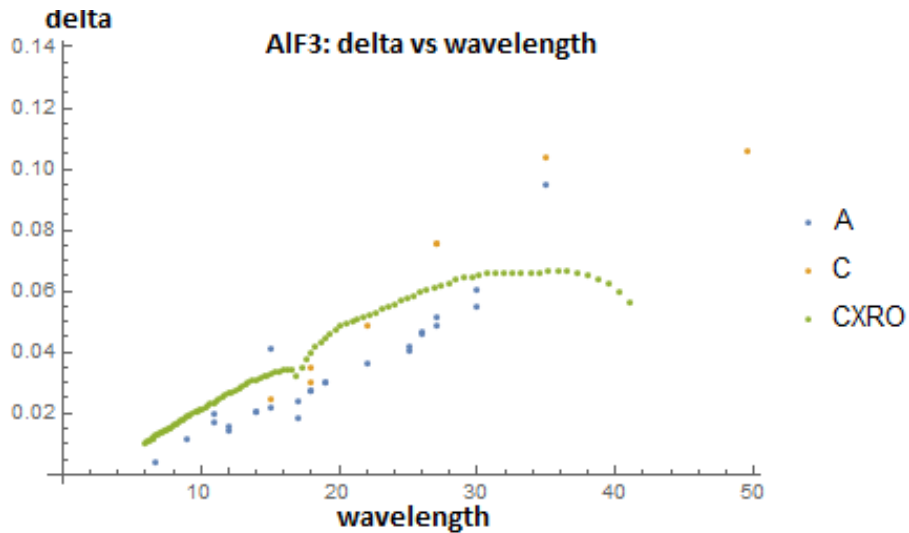


Figure 12: Structure of the Samples with an Additional Layer of Aluminum Oxyfluoride.

The thickness of both  $\text{AlF}_3$  and  $\text{AlF}_2\text{O}$  should be equivalent to the thickness of the single  $\text{AlF}_3$  layer in the original model. For this adjustment in the model, we only need to focus on the

thicker samples. This change would cause thin samples, like sample D, to have only a layer of  $\text{AlF}_2\text{O}$  and no  $\text{AlF}_3$  layer. Therefore since we are primarily interested in the  $\text{AlF}_3$ , we only refitted samples A and C (day 1) with this modification. The model was run two times like in the original fit: once to predict the thickness and the second to predict the index of refraction. We estimated that the  $\text{AlF}_2\text{O}$  was 30 Angstroms thick. The model predicted the thickness of the  $\text{AlF}_3$  for sample A was 49 Angstroms and for sample C 51 Angstroms. This makes the total thickness of the two layers 79 Angstroms and 81 Angstroms for samples A and C respectively. The thickness for A differs by 38%, but for C only differs by 3% from the experimental averages of the original model. The resulting graphs of index of refraction vs. wavelength with this added layer are in Figure 13.



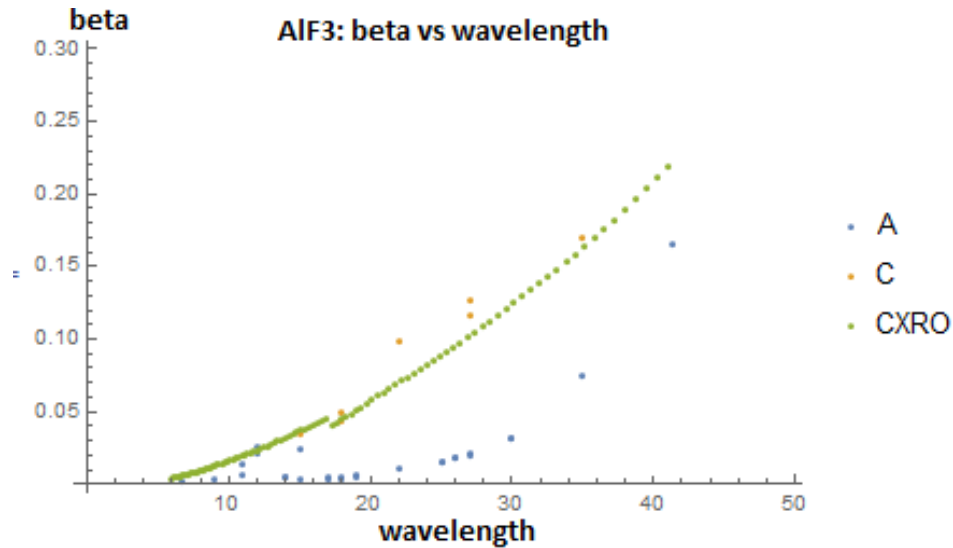


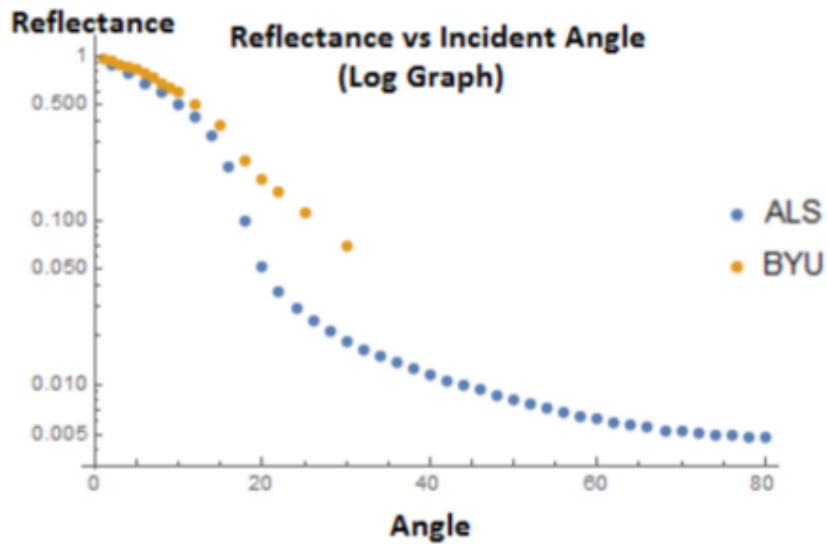
Figure 13: Graphs of Delta and Beta vs. Wavelength (nm) of the Data Modeled with a Second Layer Compared to the CXRO Data.

With a second layer, the experimental data does not match the CXRO data even for the shorter wavelengths. Both samples are spread out and do not have values close to each other.

Because the data does not fit as nicely with the CXRO data, it is not surprising that after a closer look at the samples it was concluded that a second layer of AlF<sub>2</sub>O was not necessary. Moreover, this second modification did not improve the fit either. The original fit will be used in the comparison with the BYU data because it is the most accurate one.

### 3.2 ALS and BYU Data Comparison

At BYU, we measured sample D at wavelengths 25.63 nm and 30.4 nm. Ideally the measurements should be the same or similar to the data taken at the ALS because it is the same sample. However, as seen in Figure 14, the measurements are not the same.



ALS	Estimate	Standard Error	BYU	Estimate	Standard Error
ndx	0.928176	0.000223861	ndx	0.830701	0.00993142
beta	0.0734126	0.000640469	beta	0.291319	0.0248351

Figure 14: Comparison of ALS and BYU Data for Sample D at 25.6 nm. The graph is reflectance vs. incident angle (degrees). The tables below the graph compare the index of refraction, the real part  $ndx$  and the imaginary part  $beta$ .

At the wavelength of 25.6 nm, the reflectance recorded at BYU for higher angles is larger than the reflectance recorded at the ALS. Even at the lower angles, the reflectance is higher for the BYU measurements. The index of refraction is also different: at BYU we calculated a lower  $n$  and a higher  $beta$  than at the ALS. Another difference is the standard error is lower for the ALS data. These discrepancies are also seen at a wavelength of 30.4 nm in Figure 15.

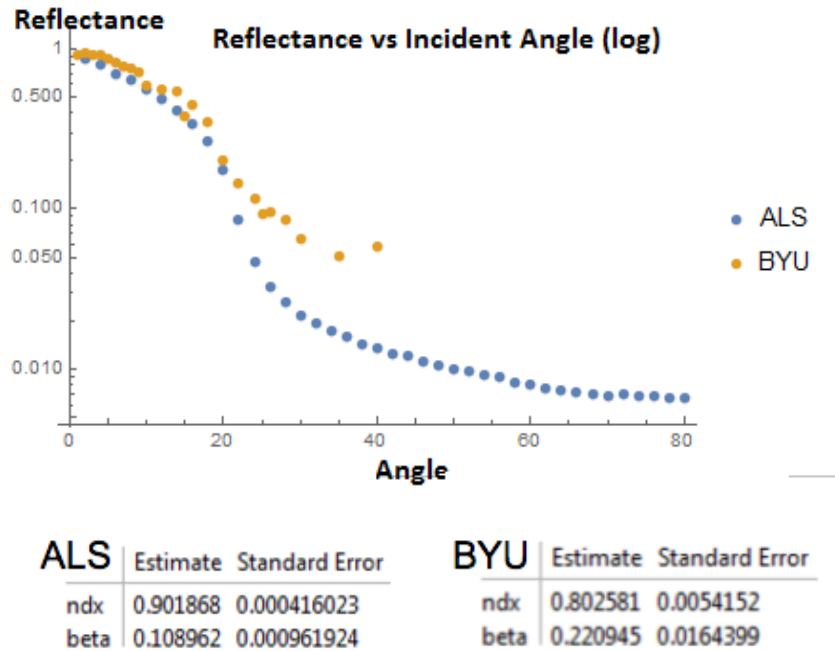


Figure 15: Comparison of ALS and BYU Data for Sample D at 30.4 nm. The graph is reflectance vs. incident angle (degrees). The tables below the graph compare the index of refraction, the real part  $ndx$  and the imaginary part  $beta$ .

At a wavelength of 30.4 nm, the reflectance for higher angles is larger at BYU as well. The  $n$  is lower and the  $beta$  is higher for the BYU measurements. Additionally, the standard error for the BYU data is higher than the ALS data. This change in reflectance and index of refraction is puzzling. If the sample was somehow damaged or the sample oxidized between the ALS measurements and BYU measurements, then reflectance should have gone down. An increase in reflectance indicates that there is a difference between the two systems. At first, we considered if the noise in the BYU lab was properly accounted for. Yet after further investigation, we concluded that the noise was negligible. We are currently having a problem with the detector, where the counts dramatically drop over time. This might be the source of the problem, but for now nothing is definite.

### 3.3 Conclusion and Future Work

We were successful in taking data at the ALS and at BYU. Getting the system configured and operating in the BYU lab is a great accomplishment because now students will be able to focus fully their research this fall semester and not worry about alignment. The measurements we took at the ALS agree nicely with the CXRO data. It turned out that our original fit was the most accurate one, despite our attempts to improve it. Work still needs to be done on identifying why the measurements from the ALS are different than the BYU measurements. The current plan is to switch the detector with another one. This might solve our problems with the detector counts and the high reflectance measurements.

We would like to publish a paper this fall on our findings: the index of refraction of  $\text{AlF}_3$  from 13 nm to 49.5 nm. Hopefully the paper will add to the work of Bridou and other scientists from the Charles Fabry Laboratory of the Optics Institute. Figure 16 shows our data compared to the data from Bridou's experiment. Although there is a gap between 50 nm and 60 nm, we were able to fill in information for the lower wavelengths in the EUV spectrum that has not been determined before.

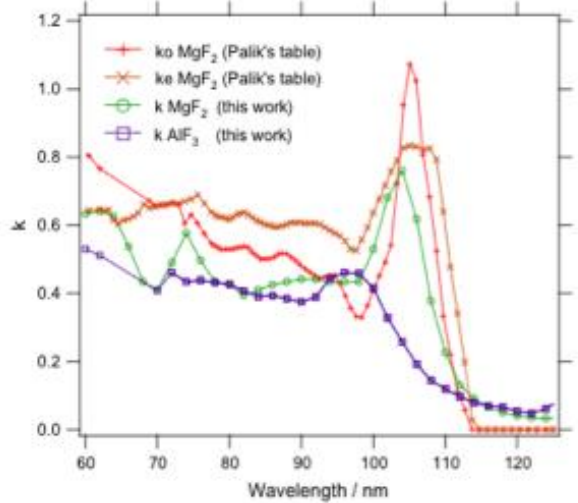
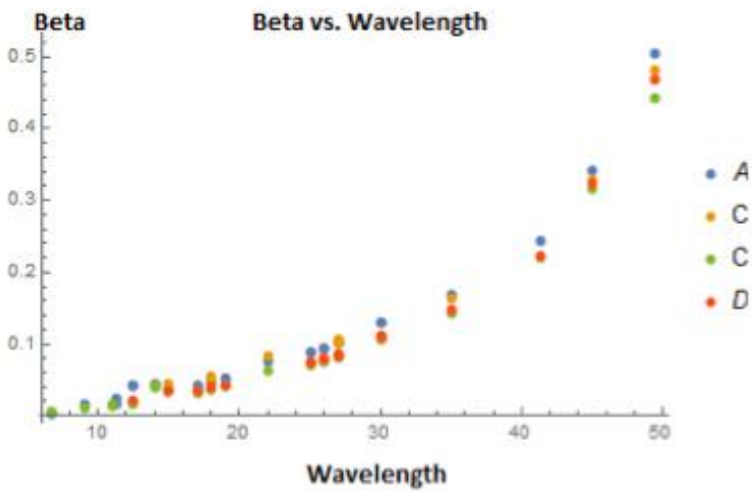
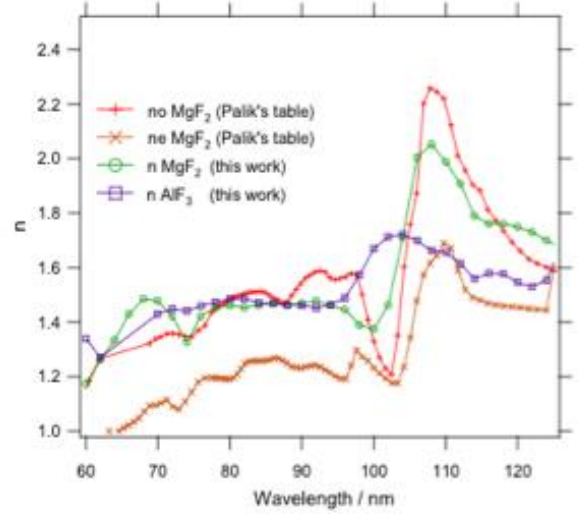
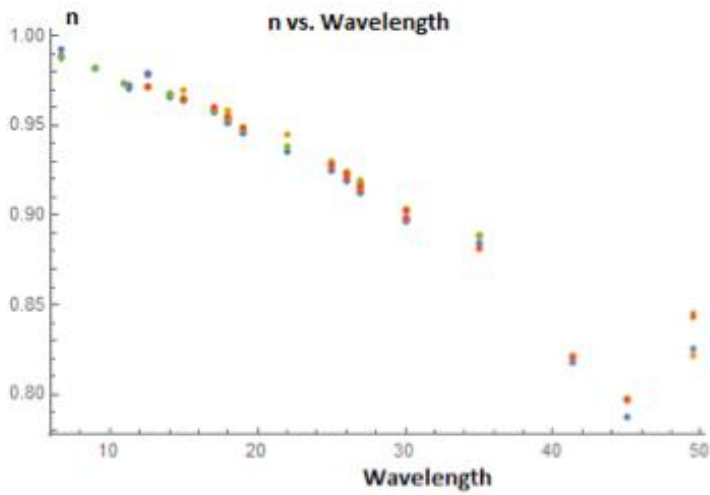


Figure 16: Comparison of our experimental data (left) with Bridou's data (right) [2]. The top graphs are  $n$  vs. wavelength (nm) and the bottom graphs are  $beta$  (or  $k$ ) vs. wavelength (nm). In Bridou's graphs, we are only interested in the purple squared line that represents the  $AlF_3$ .

## References

- [1] C.S. Moore, J. Hennessy, E. Kersgaard, A.D. Jewell, S. Nikzad, and K. France, UV, X-Ray, and Gamma-Ray Space Instrumentation for Astronomy XIX (2015).
- [2] F. Bridou, M. Cuniot-Ponsard, J.-M. Desvignes, M. Richter, U. Kroth, and A. Gottwald, Optics Communications **283**, 1351 (2009).
- [3] J. Peatross and M. Ware, *Physics of Light and Optics* (Brigham Young University, Dept. of Physics, Provo, UT, 2011).
- [4] D.T. Attwood, *Soft x-Rays and Extreme Ultraviolet Radiation: Principles and Applications* (Cambridge University Press, Cambridge, 2000).
- [5] “X-Ray Interactions with Matter”, *The Center for X-Ray Optics*, [http://henke.lbl.gov/optical\\_constants/](http://henke.lbl.gov/optical_constants/) (8 August 2016).

## List of Figures

<b>Figure 1:</b> Snell’s Law and the Law of Reflection. _____	4
<b>Figure 2:</b> BYU Setup. _____	6
<b>Figure 3:</b> Reflectance vs. Incident Angle for Sample A for 45 nm. _____	8
<b>Figure 4:</b> Layers of the Sample Mirror. _____	9
<b>Figure 5:</b> Thickness (Angstroms) vs. Wavelength (nm) for Sample A. _____	10
<b>Figure 6:</b> Fitted Graph for Sample A at 45 nm. _____	11
<b>Figure 7:</b> Fitted Graph for Sample A at 6.7 nm. _____	11
<b>Figure 8:</b> Graphs of n, Delta, and Beta vs. Wavelength (nm). _____	14
<b>Figure 9:</b> Comparison of Delta and Beta vs. Wavelength (nm) Graphs of ALS Data with CXRO Data. _____	15
<b>Figure 10:</b> Table of the Thicknesses. _____	17
<b>Figure 11:</b> Graphs of Delta and Beta vs. Wavelength (nm) of the Data Modeled with the Predicted Thicknesses Compared to the CXRO Data. _____	17
<b>Figure 12:</b> Structure of the Samples with an Additional Layer of Aluminum Oxyfluoride. ____	18
<b>Figure 13:</b> Graphs of Delta and Beta vs. Wavelength (nm) of the Data Modeled with a Second Layer Compared to the CXRO Data. _____	20
<b>Figure 14:</b> Comparison of ALS and BYU Data for Sample D at 25.6 nm. _____	21
<b>Figure 15:</b> Comparison of ALS and BYU Data for Sample D at 30.4 nm. _____	22
<b>Figure 16:</b> Comparison of our experimental data with Bridou’s data _____	24